Modified Shepard interpolation method applied to trapping mediated adsorption dynamics

P. N. Abufager,[a] C. Crespos[b] and H. F. Busnengo*[a]

Received 24th November 2006, Accepted 13th February 2007
First published as an Advance Article on the web 7th March 2007
DOI: 10.1039/b617209a

The modified Shepard (MS) interpolation method is applied to H_2/Pd(111) to investigate its performance for a system for which dissociative adsorption takes place through a direct as well as an indirect (*i.e.* dynamic trapping) mechanism. The input data were obtained from an available accurate potential energy surface (PES) interpolated by using the corrugation reducing procedure (CRP). Dissociation probabilities obtained from classical trajectory calculations with the MS-PES are in very good agreement with the results for the CRP-PES. Thus, this study confirms the MS method as a promising tool to tackle low energy adsorption dynamics of polyatomic molecules, usually dominated by trapping.

1. Introduction

Nowadays molecule–surface interactions are theoretically studied through the analysis of the corresponding potential energy surface (PES) obtained, in general, from state-of-the-art electronic structure calculations[1–4] based on density functional theory (DFT). Due to their computational cost, these calculations are carried out for some selected molecular configurations considered as the most relevant ones for the process of interest. However, dynamic simulations require values of the potential and forces for a great number of molecular configurations. Therefore, an accurate continuous representation of the PES obtained by interpolation or fitting of a reduced set of DFT data is highly desirable. Thus, in the last decade, various interpolation and fitting methods have been proposed and implemented for molecule–metal surface reactions.[5–14]

The corrugation reducing procedure (CRP)[8] is an accurate interpolation method which has been successfully employed for diatomic molecules interacting with several metal surfaces.[8,9,15–23] However, its extension to deal with polyatomic molecules is not straightforward. More recently, the modified Shepard (MS) interpolation method, developed in the framework of gas phase reactions by Collins and co-workers,[24–32] was adapted for molecule–surface interactions.[10,11] In the MS method, the PES is expressed as a weighted series of second order Taylor expansions centered at data points scattered throughout the configuration space. This set of points will be referred to as the PES data set. The PES data set is grown up through an iterative procedure that adds points in regions of the configuration space important for the dynamics until convergence of the reaction probability of interest is achieved.[32] Thus, in contrast with other interpolation methods, the MS method does not require a regular grid of data points and optimizes the requirement of DFT calculations. Moreover, what makes the MS method more promising is that it allows to deal with polyatomic molecules.[33]

For molecule–surface interactions, the MS method is still under development. On one hand, some methodological issues related with the symmetry properties of the MS-PES have not yet been investigated in depth (see section 2.2). On the other hand, the MS method has been so far employed for H_2/Pt(111)[10,11] and N_2/Ru(0001)[34,35] for which dissociative adsorption is a direct activated process. A very good performance of the MS method was obtained in both cases, providing accurate dynamical results from relatively small PES data sets.[10,11,34] Nevertheless, even for diatomic molecules, the adsorption dynamics is often more complex than the one encountered for direct activated processes (*e.g.* H_2/Pd, N_2/W, *etc.*).[15,20] In the case of H_2/Pd(111), dissociative adsorption takes place through both, a direct and an indirect (*i.e.* dynamic trapping) mechanism.[36] Direct dissociation dominates at high energies while dynamic trapping plays a prominent role at low energies. In fact, it is the interplay between direct and dynamic trapping mediated adsorption responsible for the non-monotonous behavior of the sticking probability as a function of collision energy[15,37] and its dependence on the angle of incidence[38] found in molecular beam experiments.[39] A key practical difference between H_2/Pt(111) and N_2/Ru(0001) on one hand and H_2/Pd(111) on the other, is that in the latter case, the sticking probability is large even at very low energies (*e.g.* below 50 meV) because dissociative adsorption is non activated. Then, dealing with H_2/Pd(111) one is specially interested in the low energy regime (accessible for room temperature effusive beam experiments and in work conditions of most catalytic reactions) in which two different reaction mechanisms are simultaneously operative and the

[a] *Instituto de Física Rosario, IFIR, (CONICET-UNR) and Facultad de Ciencias Exactas, Ingeniería y Agrimensura, Universidad Nacional de Rosario, Av. Pellegrini 250, 2000 Rosario, Argentina. E-mail: busnengo@ifir.edu.ar*
[b] *Laboratoire de Physico-Chimie Moléculaire, UMR 5803 CNRS—Université Bordeaux I, 351 Cours de la Libération, 33405 Talence Cedex, France*

dynamics is highly sensitive to small variations of the PES.[15] Such a system represents a challenge for the MS method, also because trapped molecules explore a larger region of the configuration space than in the case of direct scattering. Our aim is to gauge the performance of the MS method to deal with non-activated processes dominated by dynamic trapping: a crucial issue for future extensions of the MS method for adsorption of polyatomic molecules for which it is well known that indirect mechanisms usually play a prominent role.[40,41]

In the present work the MS scheme is applied to H_2/Pd(111) and, like in ref. 10 and 11, we take advantage of an available accurate CRP-PES[15] for a fast evaluation of the potential and its derivatives (*i.e.* the input data) required in the MS-PES growing process. More information about the accuracy of the CRP interpolation method for H_2/Pd(111) and the DFT calculations used to build the CRP-PES can be found in ref. 15 and 42, respectively. The paper is set as follows. Sections 2.1 and 2.3 briefly describe the general features of the MS method and the classical trajectory calculations we have used in the growing process, respectively. In section 2.2 we present an original and detailed discussion about the symmetry properties of molecule–surface MS-PESs considering, in particular, the existence and origin of discontinuities of their derivatives. In section 3, we present the results of the MS-PES growing process and dissociative adsorption probabilities considering the contribution of both direct and dynamic trapping mechanisms. The accuracy of the MS method is analyzed by comparing the dynamical results obtained with MS-PES and CRP-PES. The performance of the MS method for H_2/Pd(111) is compared with the one for H_2/Pt(111)[10,11] taking into account the size of the PES data sets required for well converged dynamical results. Finally, a quantitative evaluation of the derivative discontinuities of the MS-PES is presented and their effects on the dynamics are also addressed. In section 4 we summarize the conclusions of our study.

2. Methods and computational details

2.1 The MS method

In the framework of the MS method,[24,25] the PES is given by a weighted series of Taylor expansions centered at data points sampled throughout the configuration space. For a diatomic molecule impinging on a *frozen* surface, we deal with a six-dimensional configuration space. For a configuration described by the vector $\boldsymbol{\xi} = (\xi_1,\xi_2,\cdots,\xi_6)$, the potential $V(\boldsymbol{\xi})$ is given by

$$V(\boldsymbol{\xi}) = \sum_{i=1}^{N_{\text{data}}} w_i(\boldsymbol{\xi}) T_i(\boldsymbol{\xi}). \qquad (1)$$

Following ref. 10 and 11, the coordinates $\xi_1,\xi_2,\cdots,\xi_6$ are defined as linear combinations of the inverse interatomic distances between the H atoms and three Pd atoms of the surface (placed on sites A, D and F of Fig. 1) and the H–H distance, using the singular value decomposition method.[32] In eqn (1) $T_i(\boldsymbol{\xi})$ is the second order Taylor expansion of the potential centered on the data point $\boldsymbol{\xi}(i)$,

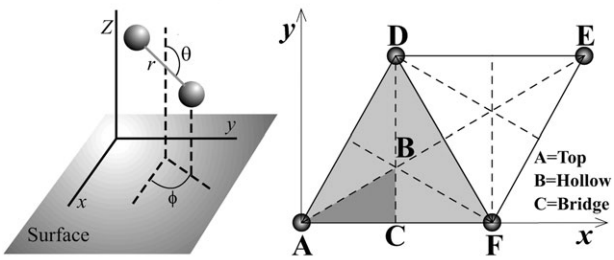

Fig. 1 Coordinate system used for the H_2/Pd(111) dynamics and definition of surface sites.

$$T_i(\boldsymbol{\xi}) = V[\boldsymbol{\xi}(i)] + \sum_{k=1}^{6}[\xi_k - \xi_k(i)]\left.\frac{\partial V}{\partial \xi_k}\right|_{\xi(i)} + \frac{1}{2}\sum_{k=1}^{6}\sum_{j=1}^{6}[\xi_k - \xi_k(i)][\xi_j - \xi_j(i)]\left.\frac{\partial^2 V}{\partial \xi_k \partial \xi_j}\right|_{\xi(i)}, \qquad (2)$$

with $\{\boldsymbol{\xi}(1),\boldsymbol{\xi}(2),\cdots,\boldsymbol{\xi}(N_{\text{data}})\}$ being the PES data set. The form of the weight function, w_i, employed here is the same as in ref. 11. The MS method requires the calculation of energy, its gradient and second derivatives for all the data points $\boldsymbol{\xi}(i)$. The initial PES data set is built by choosing molecular configurations close to some possible reaction pathways. Then, it is iteratively grown up by adding points in regions of the configuration space where an accurate determination of the potential is required. A single iteration cycle consists in running classical trajectory calculations to select and add new molecular configurations to the PES data set, which is then used for an accurate evaluation of reaction probabilities of interest. Two different criteria are used to select new molecular configurations.[10,11,24,25] The first one locates data points in regions most frequently visited by classical trajectories and the second one selects points in regions where the interpolated potential is expected to be the least accurate. The growth of the PES is stopped when the convergence of the reaction probability of interest is achieved. Further technical details concerning the coordinates and weights used can be found elsewhere.[11,24,25]

2.2 Symmetry properties of the MS-PES for molecule–surface interactions

Given a molecular configuration, $\boldsymbol{\xi}$, the set of all its symmetry equivalent configurations, $S_\xi = \{\boldsymbol{\xi}^{(1)}, \boldsymbol{\xi}^{(2)}, \boldsymbol{\xi}^{(3)},\cdots\}$, is obtained by applying the full set of symmetry transformations under which the system is invariant, $T = \{T^{(1)}, T^{(2)}, T^{(3)},\cdots\}$,

$$\boldsymbol{\xi}^{(j)} = T^{(j)}\boldsymbol{\xi}, \quad j = 1,2,3,... \qquad (3)$$

Accordingly, a set of configurations S, is considered symmetric under the transformation $T^{(k)}$ if $\forall\boldsymbol{\xi} \in S$, $\boldsymbol{\xi}^{(k)} \in S$, and fully symmetric if $\forall\boldsymbol{\xi} \in S$, $S_\xi \subset S$. Using the MS method, the correct symmetry properties of the PES are ensured if the PES data set is fully symmetric. For systems composed by a finite number of atoms (*e.g.* gas phase reactions), $\forall\boldsymbol{\xi}$, S_ξ has a finite number of elements which can be easily obtained by

permutation of identical atoms of the system.[24,25] However, for gas–surface reactions, the system is composed by infinite (surface) atoms and $\forall\xi$, S_ξ has an infinite number of elements being impossible (in practice) to work on using a fully symmetric PES data set. Therefore, the symmetry properties of the molecule–surface PES obtained with the MS method must be considered with caution.

From now on, we will restrict our analysis to the case of a homonuclear diatomic molecule interacting with the (111) surface of a face centered cubic (FCC) crystal (Fig. 1), the generalization for other surfaces and/or molecules being straightforward. We will also asume C_{6v} symmetry of the surface which is a good approximation for H_2 interacting with several FCC(111) metal surfaces.[16]

Due to the symmetry properties of a FCC(111) surface, for any configuration ξ, there exists a configuration $\xi^{(k)} \in S_\xi$, whose molecular center is located within the triangle ABC (see Fig. 1). Therefore, the potential $V(\xi)$ and its derivatives can be computed by evaluating $V(\xi^{(k)})$ and its derivatives. Thus, the resulting PES is invariant under all the symmetry transformations of the system. Still, special care must be exercised when its derivatives are considered, in particular on the edges of the triangle ABC. In the previous implementations of the MS method for gas–surface reactions,[10,11,34] the PES data set was composed by configurations ξ whose molecular center was within the triangle ADF (see Fig. 1). Thus, the PES data set is not fully symmetric. It is, for instance, symmetric under reflection with respect to the lines AB, BC and BF but not under reflection with respect to the line AC. This entails symmetry-inconsistent values of some derivatives of the PES for configurations with the molecular center right above the line AC and all its symmetry equivalent lines (hereafter referred to as *problematic lines*). This provokes discontinuities of the derivatives whenever the center of the molecule crosses one of these lines (*e.g.* AD, AF, DF, *etc.*). For instance, for molecular configurations parallel to the x-axis (*i.e.* $\theta = 90°$, $\phi = 0°$), $\partial V/\partial y_{cm}$ in general, does not go exactly to zero when $y_{cm} \rightarrow 0^+$, *i.e.*, $\lim_{ycm\rightarrow 0^+} \partial V/\partial y_{cm} = -\lim_{ycm\rightarrow 0^-} \partial V/\partial y_{cm} \neq 0$. Therefore, the PES is not well behaved and difficulties do appear in dynamical calculations whenever the center of the molecule crosses one of these problematic lines.

In ref. 10, 11 and 34 this problem was avoided restricting the dynamics to the region ADF by using the standard reflection algorithm, often employed in molecular dynamics simulations to account for periodicity. This procedure works well for H_2/Pt(111). This might be because derivative discontinuities are very small or because direct scattering mechanisms entail a small number of crossing of problematic lines.

When dynamic trapping is important, the discontinuity of the derivatives along the problematic lines might become a more serious problem. For H_2/Pd(111), at low energies, a large fraction of trajectories are trapped and explore a large surface area before dissociation or reflection. Thus, the effect of artificially reflecting the trajectories whenever they reach the edges of the triangle ADF, might introduce a distortion of the classical trajectories and deteriorate the efficiency of the growing process. Moreover, by using the reflection algorithm the problem of the derivative discontinuities is completely hidden and it is not possible to quantify the effect on the dynamics of reflecting the trajectories on the problematic lines. In this paper we have implemented an alternative procedure. We have also used a PES data set restricted to the region ADF like in ref. 10 and 11. However, in the dynamical calculations we have allowed the trajectories to cross the problematic lines. When during a crossing, total energy is not conserved (due to discontinuities of the derivatives), we have scaled the kinetic energy (without changing the direction of the velocity of each atom) to preserve the total energy of the system. This allows a quantitative evaluation of the effect of the derivative discontinuities on the dynamics.

2.3 Growing process

In what follows, when the number of molecular configurations of the PES data set is given, we will only consider those whose molecular center is within the triangle ABC shown in Fig. 1. The initial PES data set is composed by 85 data points along the most favorable $2D(Z, r)$ reaction paths (Z and r are the molecule–surface and the H–H distance, respectively) for the molecule parallel to the surface centered on top, hollow and bridge sites (see Fig. 1) and for a few unreactive configurations perpendicular to the surface. For H_2/Pd(111) there exists an accurate PES constructed with the CRP method (CRP-PES).[15] In this work, the potential energy and its derivatives for each data point are obtained by using the latter CRP-PES.

It has been shown that to obtain accurate reaction probabilities over a wide range of energies, it is convenient to grow the PES data set at three energies (*i.e.* growing energies) simultaneously.[10,11] In this work, we have used the growing energies: $E_1 = 25$ meV, $E_2 = 100$ meV and $E_3 = 400$ meV. We have performed classical trajectory calculations accounting for vibrational softening through the addition of an attractive term to the PES (*i.e.* CZPE calculations).[37] This is due to the fact that dynamic trapping is quenched in the so-called quasiclassical (QC) calculations that explicitly take into account the initial vibrational zero point energy (ZPE) of the molecules.[15] We start trajectories at $Z = 6$ Å where the interaction of the molecule with the surface vanishes. We used a conventional Monte Carlo procedure to obtain a uniform random distribution of the initial x and y coordinates (Fig. 1) of the molecular center over the unit cell and the molecular orientation. The H–H distance is initially chosen equal to its equilibrium value in the vacuum (*i.e.* $r = 0.75$ Å) and $dr/dt = 0$. All the calculations were performed for $H_2(v = 0, J_i = 0)$ and normal incidence. We consider that dissociation takes place whenever r reaches the value $r_{dis} = 2.25$ Å with $dr/dt > 0$. In contrast with ref. 10, 11 and 34, to integrate the equations of motion in the classical trajectory calculations we used a variable time-step method (the predictor–corrector algorithm of Burlisch and Stoer[43]). This was necessary to ensure total energy conservation at low energies (below $\sim$ 50 meV) for which long integration times are required because of dynamic trapping.

Within the Nth iteration cycle we integrate 1500 classical trajectories and select 150 new data points to be added to the PES data set. Then, a sample of 5000 trajectories are computed and an accurate dissociation probability, P_{diss}^{MS-N}, is determined. The growing process is stopped when

$P_{diss}^{MS-(N-1)}$ and $P_{diss}^{MS-(N-2)}$ are both within the interval $[P_{diss}^{MS-N} - 0.005, P_{diss}^{MS-N} + 0.005]$ simultaneously for E_1, E_2, and E_3. In what follows, the MS-PES obtained after N iteration cycles will be referred to as MS-PES-N.

3. Results and discussions

Fig. 2 presents the dissociation probability P_{diss}^{MS-N} as a function of the number of grow iteration cycle, N, for the three initial energies used in the growing process. According to our criterion, convergence is achieved for $N = 12$, the number of molecular configurations in the corresponding PES data set being 1897.

In the present case, the accuracy of the MS method can be studied by comparing P_{diss}^{MS-12} with the "exact" dissociative adsorption probability obtained with the CRP-PES (P_{diss}^{CRP}). This comparison is presented in Fig. 3, where the contributions of direct and dynamic trapping dissociation mechanisms (P_{diss}^{dir} and P_{diss}^{trap}, respectively) are also shown. Following ref. 15, we define P_{diss}^{trapp} as the fraction of trajectories leading to dissociation after more than five rebounds and $P_{diss}^{dir} = P_{diss} - P_{diss}^{trapp}$. Fig. 3 shows that both dissociation mechanisms are very well described when the MS-PES-12 is employed, and very good agreement between P_{diss}^{MS-12} and P_{diss}^{CRP} is found in the whole energy range considered. Discrepancies between P_{diss}^{MS-12} and P_{diss}^{CRP} are lower than 1% for $E_i \geq 50$ meV and slightly increase up to ~2% at lower energies. In the latter case, P_{diss}^{MS-12} is greater than P_{diss}^{CRP} and overestimation comes from dynamic trapping mediated adsorption.

From Fig. 2 it is important to note that from the fourth iteration cycle (*i.e.* for $N \geq 4$), $|P_{diss}^{MS-N} - P_{diss}^{MS-12}|$ is lower than 0.02. Moreover, reasonably good agreement with P_{diss}^{CRP} is also obtained by using the MS-PES-4 built from a PES data set of only 700 molecular configurations (see the inset of Fig. 3). This number should be compared with the ~4000 configurations used to build the CRP-PES.[37] It must be kept in mind, however, that within the MS method, not only the potential is required but also its first and second order derivatives for each molecular configuration of the PES data set.

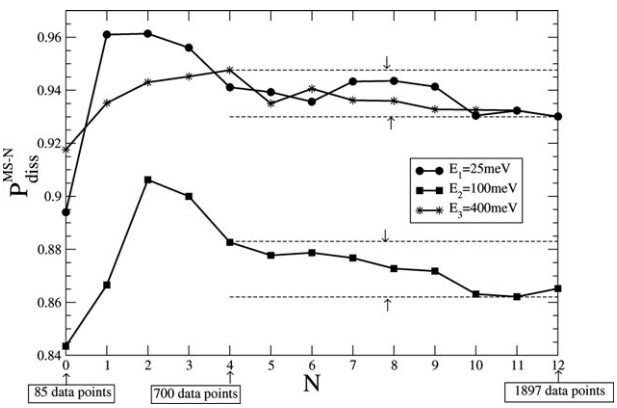

Fig. 2 Dissociative adsorption probabilities, P_{diss}^{MS-N}, for H_2/Pd(111) as a function of the number of iteration cycles, N, for energies $E_1 = 25$ meV, $E_2 = 100$ meV and $E_3 = 400$ meV.

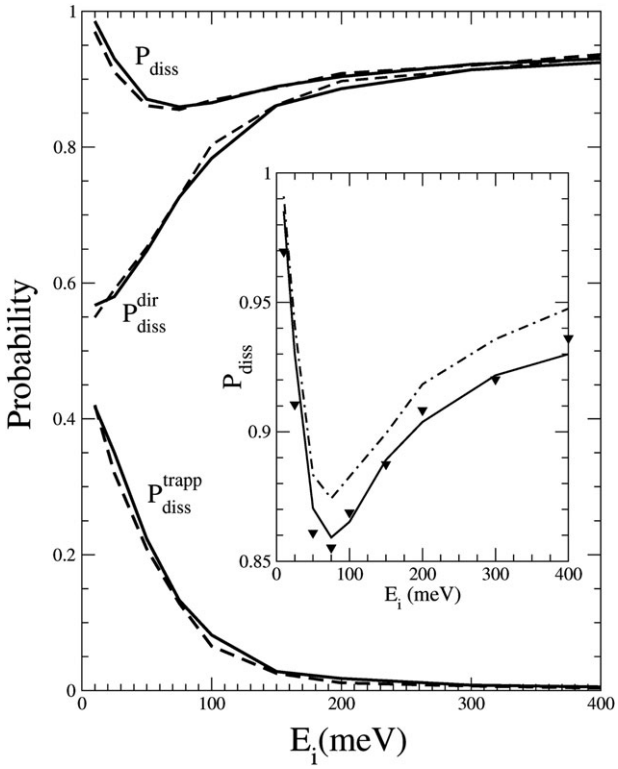

Fig. 3 Dissociative adsorption probabilities, P_{diss}^{MS-12} (solid line) and P_{diss}^{CRP} (broken line). P_{diss}^{dir} and P_{diss}^{trapp} are the contributions from the direct and dynamic trapping mechanisms. Inset: P_{diss}^{MS-12} (solid line), P_{diss}^{MS-4} (dot-dashed line) and P_{diss}^{CRP} (down triangles).

Taking into account the number of molecular configurations required for converged results within the MS method ($N = 12$) and the discrepancies between P_{diss}^{MS-12} and P_{diss}^{CRP} at low energies, it turns out that the efficiency of the MS-method for H_2/Pd(111) is slightly lower than that for H_2/Pt(111). This seems to be a consequence of the more complex dynamics which provokes a large fraction of trajectories to explore a large fraction of the configuration space. Still, it is quite difficult to trace such a small discrepancy (~2%) back to its source.

As shown in ref. 10, useful information is provided by the analysis of the molecular configurations added to the PES data set during the growing process. The values of Z and r for these molecular configurations are shown in Fig. 4. Previous dynamical studies for H_2/Pd(111), based on the CRP-PES have shown that P_{diss} is determined by the dynamics in the entrance channel.[36] Therefore, one expects that most of the configurations added to the PES data set would be placed in that region. However, only for $E_1 = 25$ meV a significant fraction of the molecular configurations added to the PES data set (17%) are in the entrance channel ($Z \geq 2$ Å) and about 98% of the configurations added for $E_3 = 400$ meV are located in the exit channel. This surprising scenario is at odds with the one found for H_2/Pt(111) where the added points are mostly located in the entrance channel (see Fig. 6 of ref. 11). This is due to the following two factors:

(i) In contrast with ref. 10 and 11, during the growing process we have carried out CZPE calculations for which the

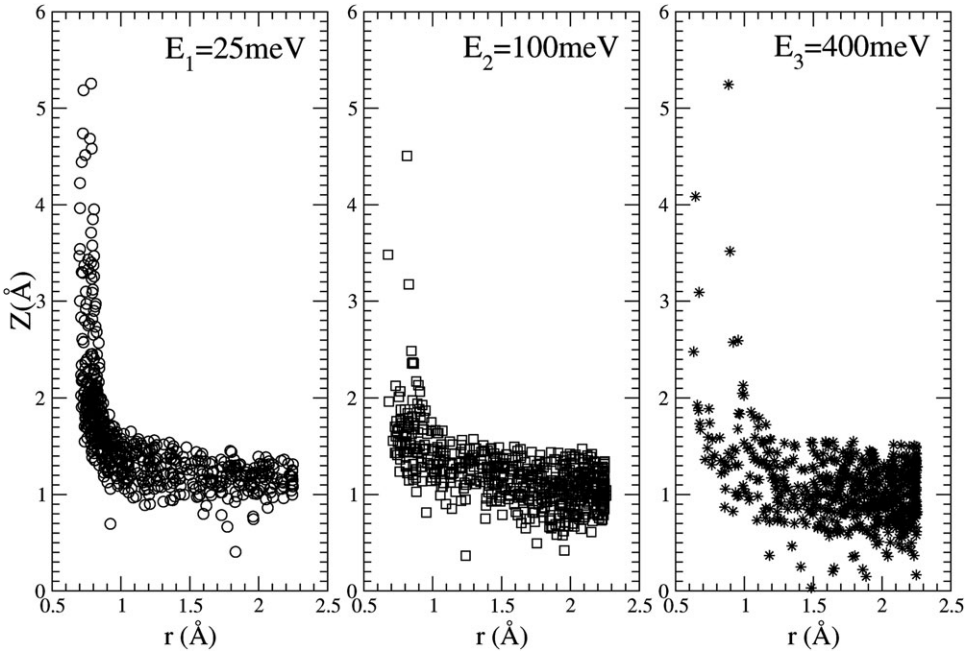

Fig. 4 2D (r,Z) representation of the molecular configurations added to the PES data set during the MS-PES growing process.

initial rovibrational energy of the incoming molecules is zero and all the molecules approach the surface with $r \approx r_{eq} =$ 0.75 Å. Then, far from the surface almost all the data points correspond to $r \approx r_{eq}$ because other values of r can only be reached by vibrationally excited reflected molecules, but the vibrational excitation probability is very small.

(ii) The higher reactivity of the H_2/Pd(111) PES makes the molecules dissociate following a much larger variety of reaction pathways than in the case of H_2/Pt(111). An evidence of this is the larger dispersion of the (Z,r) values observed for $E_3 = 400$ meV in the exit channel, compared with the case of H_2/Pt(111) (see Fig. 6 of ref. 11). Moreover, for H_2/Pd(111) almost all the trajectories visit the exit channel ($P_{diss} \approx 1$) where the PES presents a strong dependence on (and coupling between) all six molecular degrees of freedom. Thus, the two selection criteria tend to add data points in the exit channel during the growing process.

In spite of the relatively small number of data points added far from the surface, the dissociation probability is very well described by the MS method. It is interesting, however, to explore if similar good results are also obtained for the final rotational state and angular distributions of reflected molecules which evolve entirely far from the surface.

In ref. 44, it has been shown that the essential features of the scattering of H_2 on Pd(111) can be correctly described with classical calculations (including diffraction). Thus, we have followed the methods described in ref. 44 to computed CZPE rotational excitation (Fig. 5) and diffraction order probabilities (Fig. 6) by using both MS-PES-12 and CRP-PES.

In classical trajectory calculations diffraction probabilities can be estimated by dividing the reciprocal space in Wigner–Seitz cells constructed around each point of the reciprocal lattice. Diffraction probabilities are calculated by considering that trajectories with a change of parallel momentum of the molecule, $\Delta P\|$, laying within the cell centered at the end of the reciprocal lattice vector $\boldsymbol{G}_{n,m}\hbar = (n\boldsymbol{b}_1 + m\boldsymbol{b}_2)\hbar$ (with $\boldsymbol{b}_1$ and $\boldsymbol{b}_2$, the basis vectors) are associated with the (n, m) diffraction channel.[44] Then, we define diffraction order probabilities as the sum of diffraction probabilities of the same order by assuming that two diffraction peaks are of the same order if they belong to the same hexagonal ring centered around (0, 0) in the reciprocal lattice (see Fig. 6).

In Fig. 5, normalized rotational excitation probabilities P_{ref} (J_f)/P_{ref} are plotted as a function of the translational energy for $J_f = 0$, 2, 4. The agreement between MS and CRP results is excellent. A similar good agreement is also found in the case of diffraction order probabilities calculated for an initial translational energy $E_i = 75$ meV (Fig. 6) and other energies not shown here. This is a clear proof of the robustness of the MS method.

In summary, with regard to efficiency and accuracy, the MS and CRP methods both seem to be superior to other interpolation and/or fitting schemes so far employed to describe the PES of H_2 interacting with metal surfaces from electronic structure calculations. For instance, a neuronal network approach recently applied to H_2/Pd(100) required a number of input data points close to $\sim 10^4$ for a realistic dynamical description[12] and the reactive force field approximation (ReaxFF) used for H_2 interacting with Pt surfaces provided a PES which could not elucidate the low energy indirect dissociation mechanism.[14] The PES of H_2/Pd(100) has also been represented using a Tight binding Hamiltonian technique, and fitting errors within 100 meV were obtained,[7] but to our knowledge, the accuracy of this PES was not gauged through dynamical calculations. From the results obtained for H_2/Pd(111) (present work) and H_2/Pt(111),[10,11] for H_2 the efficiency of the MS method seems similar to the CRP one, with the possibility of a straightforward extension to the case

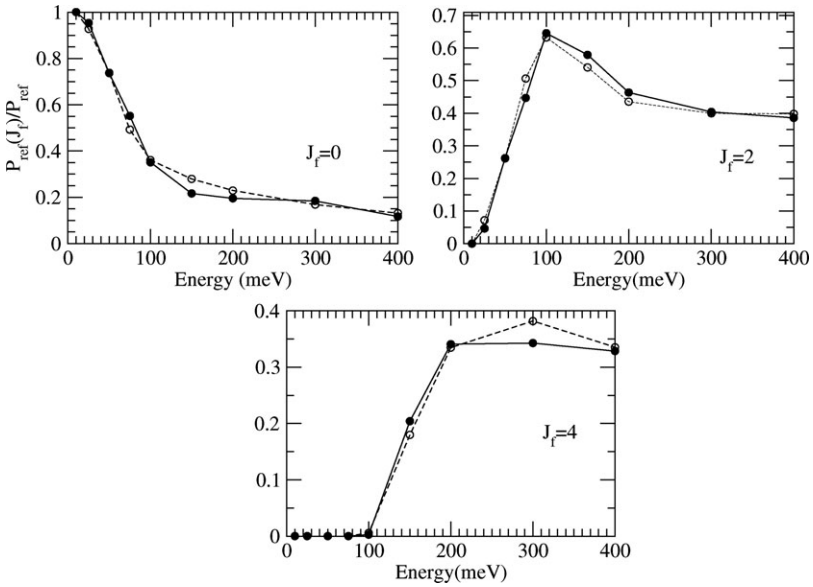

Fig. 5 Normalized rotational excitation probabilities $P_{ref}(J_f)/P_{ref}$ for $J_f = 0$, 2, 4 obtained with the MS-PES-12 (solid line) and the CRP-PES (broken line).

of polyatomic molecules being the most important advantage of the former method.

Before concluding, we address the problem of derivative discontinuity described in section 2.2. To quantify the size of this discontinuity and its effect on the dynamics, we have computed the kinetic energy change introduced to preserve total energy, ΔE_K, and the kinetic energy, E_K, whenever a crossing of a problematic line takes place. The distribution of these values for a large set of classical trajectories (for $E_i = 25$ meV) and the corresponding ratio $\Delta E_K/E_K$ are presented in Fig. 7. The relative value of the kinetic energy scaling $\Delta E_K/E_K$, is lower than 5% for the great majority ($\sim$85%) of crossings that take place during the dynamics (see Fig. 7b). Fig. 7a shows that, for instance, $\sim$80% of the kinetic energy changes introduced by the scaling procedure are lower than 5 meV whereas the kinetic energy of the molecules when the crossing takes place is, in general, greater than 50 meV. Finally, at low energies, we have compared several (initially identical) trajectories which give different results depending on the PES used in the dynamics (MS-PES or CRP-PES). We have found that the region on the surface where these trajectories start to separate from each other does not correspond to crossings of the *problematic* lines. These tests and the results of Fig. 7 strongly suggest that the derivative discontinuities of the converged MS-PES and, in particular, the kinetic energy scaling procedure we have implemented, do not influence the results of the dynamics.

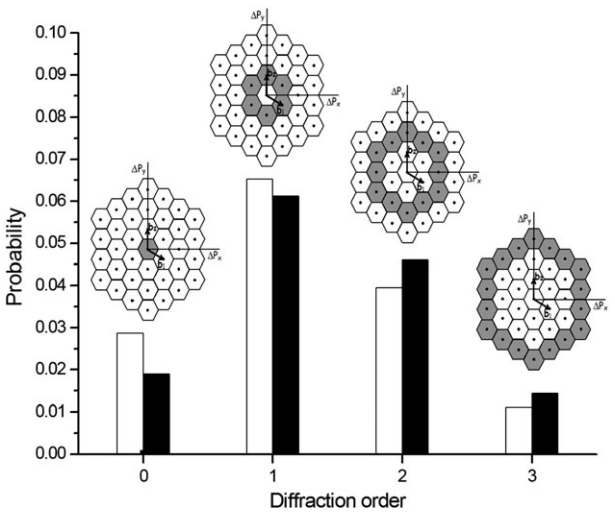

Fig. 6 Diffraction order probabilities for $E_i = 75$ meV calculated with the MS-PES-12 (full bars) and the CRP-PES (empty bars).

4. Conclusions

We have applied the modified Shepard (MS) interpolation method to H_2/Pd(111). In this case, dissociative adsorption is nonactivated and, at low energies, takes place simultaneously through both a direct and an indirect (dynamic trapping) mechanism. This entails a more complex scenario than direct single scattering processes for which the MS method has so far been applied in the framework of molecule–surface interactions. Thus, this study is relevant in view of possible future applications for other systems for which indirect mechanisms play a prominent role (*e.g.* adsorption of polyatomic molecules).

The input data for the MS method were taken from an existing accurate potential energy surface (PES) obtained from density functional theory calculations by using the corrugation reducing procedure (CRP). This allowed us to analyze the performance of the MS method by comparing classical dynamics results for the MS-PES with those obtained with the exact CRP-PES. Well converged dynamical results within the MS scheme were obtained for a PES built from $\sim$1900 input

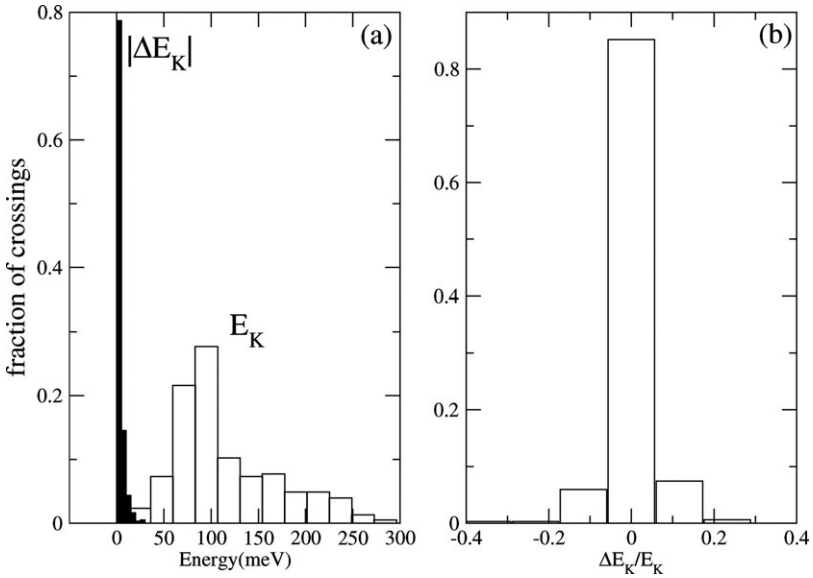

Fig. 7 (a) Distribution of the kinetic energy change introduced to preserve total energy, ΔE_K (full bars), and the kinetic energy, E_K (empty bars), whenever a crossing of a problematic line takes place. The initial energy considered is $E_i = 25$ meV. (b) Distribution of $\Delta E_K/E_K$.

molecular configuration data which means that in the present case, the efficiency of the MS-method is lower than for direct adsorption of H_2 on Pt(111) studied previously. Still, the total dissociation probability as well as the contributions of the direct and dynamic trapping mechanisms provided by a computationally cheaper MS-PES (built from $\sim$700 molecular configurations) are in good agreement with the values obtained with the CRP-PES, discrepancies being lower than 2%. Thus, this study confirms the MS method as a promising tool to tackle the problem of polyatomic molecules reacting on surfaces.

Acknowledgements

We gratefully acknowledge M. A. Collins for give us the interpolation codes developed in his group. This work has been supported by CONICET (project N° PIP 5248) and by the bilateral Argentina-France ECOS-Sud (project N° A03E04).

References

1 A. Gross, *Surf. Sci. Rep.*, 1998, **32**, 291.
2 A. Gross, *Theoretical Surface Science*, Springer, Berlin, 2003.
3 G. Kroes, *Prog. Surf. Sci.*, 1999, **60**, 1.
4 G. J. Kroes and M. F. Somers, *J. Theor. Comput. Chem.*, 2005, **4**, 493.
5 J. McCreery and J. G. Wolken, *J. Chem. Phys.*, 1975, **63**, 2340.
6 J. McCreery and J. G. Wolken, *J. Chem. Phys.*, 1977, **67**, 2551.
7 A. Gross, M. Scheffler, M. Mehl and D. Papaconstantopoulos, *Phys. Rev. Lett.*, 1999, **82**, 1209.
8 H. F. Busnengo, A. Salin and W. Dong, *J. Chem. Phys.*, 2000, **112**, 7641.
9 G. Kresse, *Phys. Rev. B*, 2000, **62**, 8295.
10 C. Crespos, M. A. Collins, E. Pijper and G. J. Kroes, *Chem. Phys. Lett.*, 2003, **376**, 566.
11 C. Crespos, M. A. Collins, E. Pijper and G. J. Kroes, *J. Chem. Phys.*, 2004, **120**, 2392.
12 S. Lorenz, M. Scheffler and A. Gross, *Physica B (Amsterdam)*, 2006, **73**, 115431.
13 A. Gross, A. Eichler, J. Hafner, M. Mehl and D. Papaconstantopoulos, *J. Chem. Phys.*, 2006, **124**, 174713.
14 J. Ludwig, D. Vlachos, A. C. T. van Duin and W. A. Goddard III, *J. Phys. Chem. B*, 2006, **110**, 4274.
15 H. F. Busnengo, C. Crespos, W. Dong, J. C. Rayez and A. Salin, *J. Chem. Phys.*, 2002, **116**, 9005.
16 R. Olsen, H. F. Busnengo, A. Salin, M. F. Somers, G. J. Kroes and E. J. Baerends, *J. Chem. Phys.*, 2002, **116**, 3841.
17 M. A. Di Césare, H. F. Busnengo, W. Dong and A. Salin, *J. Chem. Phys.*, 2003, **118**, 11226.
18 R. A. Olsen, D. A. McCormack and E. J. Baerends, *Surf. Sci.*, 2004, **571**, L325.
19 P. Rivière, H. F. Busnengo and F. Martín, *J. Chem. Phys.*, 2004, **121**, 751.
20 G. Volpilhac and A. Salin, *Surf. Sci.*, 2004, **556**, 129.
21 J. K. Vincent, R. A. Olsen, G. J. Kroes, M. Luppi and E. J. Baerends, *J. Chem. Phys.*, 2005, **122**, 044701.
22 A. Salin, *J. Chem. Phys.*, 2006, **124**, 104704.
23 M. Alducin, R. Diez Muiño, H. F. Busnengo and A. Salin, *Phys. Rev. Lett.*, 2006, **97**, 056102.
24 J. Ischtwan and M. A. Collins, *J. Chem. Phys.*, 1994, **100**, 8080.
25 K. C. Thompson and M. A. Collins, *J. Chem. Soc., Faraday Trans.*, 1997, **93**, 871.
26 R. P. A. Bettens, T. Hansen and M. A. Collins, *J. Chem. Phys.*, 1999, **111**, 6322.
27 R. O. Fuller, R. P. A. Bettens and M. Collins, *J. Chem. Phys.*, 2001, **114**, 10711.
28 A. J. Chalk, S. Petrie, L. Radom and M. A. Collins, *J. Chem. Phys.*, 2000, **112**, 6625.
29 R. P. A. Bettens and M. A. Collins, *J. Chem. Phys.*, 1998, **109**, 9728.
30 M. A. Collins and D. H. Zhang, *J. Chem. Phys.*, 1999, **111**, 9924.
31 D. H. Zhang, M. A. Collins and S. Y. Lee, *Science*, 2000, **290**, 961.
32 M. Collins, *Theor. Chem. Acc.*, 2002, **108**, 313.
33 K. Song and M. A. Collins, *Chem. Phys. Lett.*, 2001, **335**, 481.
34 C. Díaz, J. K. Vincent, G. P. Krishnamohan, R. A. Olsen, G. J. Kroes, K. Honkala and J. K. Norskov, *Phys. Rev. Lett.*, 2006, **96**, 096102.
35 R. Harrevelt, K. Honkala, J. K. Norskov and U. Manthe, *J. Chem. Phys.*, 2005, **122**, 234702.

36 C. Crespos, H. F. Busnengo, W. Dong and A. Salin, *J. Chem. Phys.*, 2001, **114**, 10954.
37 H. F. Busnengo, E. Pijper, G. J. Kroes and A. Salin, *J. Chem. Phys.*, 2003, **119**, 12553.
38 C. Díaz, H. F. Busnengo, F. Martín and A. Salin, *J. Chem. Phys.*, 2003, **118**, 2886.
39 C. Resch, H. F. Berger, K. D. Rendulic and E. Bertel, *Surf. Sci.*, 1994, **316**, L1105.
40 J. F. Weaver, A. F. Carlsson and R. J. Madix, *Surf. Sci. Rep.*, 2003, **50**, 107.
41 F. Schreiber, *Prog. Surf. Sci.*, 2000, **65**, 151.
42 W. Dong and J. Hafner, *Phys. Rev. B*, 1997, **56**, 15396.
43 J. Stoer and R. Burlisch, *Introduction to Numerical Analysis*, Springer, New York, 1980.
44 C. Díaz, M. Sommers, G. Kroes, H. Busnengo, A. Salin and F. Martín, *Phys. Rev. B*, 2005, **72**, 035401.